PRELIMINARY STUDIES ON THE INSERTION DEVICE COMPENSATION SCHEME FOR SOLEIL II

Z. Zhang*, P. Brunelle, V. Gubaidulin, S. Habet, Y. Huang[1], A. Loulergue, O. Marcouillé, L. S. Nadolski, M. Valléau, Synchrotron SOLEIL, Saint-Aubin, France
[1]also at University of Science and Technology of China, Hefei, China

Abstract

A substantial fraction of the insertion devices (IDs) installed in SOLEIL will remain in operation during the first phase of the SOLEIL II project. Studies of their impact on the upgraded lattice have been initiated in order to define the preliminary technical requirements for compensation. In this paper, the ID-induced focusing and coupling effects are characterized, followed by investigations of both Linear Optics from Closed Orbit (LOCO) and local feedforward correction schemes. Closed-orbit correction studies are performed based on measurements of the distortions generated by existing IDs on the SOLEIL storage ring and their transfer to the SOLEIL II lattice.

INTRODUCTION

SOLEIL is the French third-generation synchrotron light source, routinely operated for external users since 2008 with twenty ID beamlines [1]. The storage ring of its upgrade project, SOLEIL II, features a lattice composed of alternating 7BA and 4BA high-order achromat cells, providing an ultra-low natural horizontal emittance of about 90 pm rad at a beam energy of 2.75 GeV [2–7]. Such performance is achieved through strong transverse focusing and large bending radii in the dipole magnets, which help suppress dispersion in the arcs. As a consequence, the nonlinear beam dynamics becomes more sensitive to ID perturbations. Therefore, in addition to the closed-orbit feedforward compensation already implemented at SOLEIL [8], dedicated compensation schemes for ID-induced focusing and coupling effects will also be required for SOLEIL II, as already investigated at several other facilities [9–11].

The main parameters of the SOLEIL II bare lattice are summarized in Table 1. The Touschek lifetime was calculated for a total beam current of 500 mA distributed over 416 bunches, assuming a zero-current bunch length of 2.71 mm and an emittance ratio of 30 % [12,13]. The lattice accommodates nineteen IDs foreseen for the first and second phases of SOLEIL II [14, 15]. The Phase 1 IDs include six In-Vacuum Undulators (IVUs), one In-Vacuum Wiggler (IVW), three Cryogenic Permanent Magnet Undulators (CPMUs), eight Elliptically Polarized Undulators (EPUs), generically referred to as Helical Undulators (HUs) of APPLE-II type, and one long Adjustable Phase Undulator (APU). Sixteen of these devices are currently operated in SOLEIL and are expected to operate at smaller minimum gaps in SOLEIL II.

* zhandong.zhang@synchrotron-soleil.fr

Table 1: Main Parameters of the SOLEIL II Bare Lattice

Parameter	Value
Beam energy [GeV]	2.75
Circumference [m]	353.98
Natural emittance [pm rad]	90.5
Betatron tune ν_x / ν_y	54.2016 / 18.3011
Chromaticity Q'_x / Q'_y	1.8 / 1.4
Bunch length [mm][a]	2.71
ID capacity	19
Touschek lifetime [h][b]	3.5

[a] at zero current
[b] calculated without bunch lengthening

To define the technical requirements for ID compensation of SOLEIL II, preliminary studies of ID effects on the upgraded lattice have been initiated. Second-order kick maps of the IDs were calculated using the code `RADIA` [16] and then implemented into the bare lattice to evaluate their linear and nonlinear effects with the `Accelerator Toolbox` (`AT`) [17–19]. The impact on the on-momentum dynamic aperture was found to remain acceptable, whereas the Touschek lifetime was significantly reduced [5]. As a first step, the LOCO algorithm [20] was applied to assess the potential recovery of the Touschek lifetime in the presence of IDs. This paper presents updated ID-induced focusing and coupling effects and their global LOCO correction based on the latest version of the SOLEIL II lattice, together with a local correction scheme considered more practical for feedforward compensation. Closed-orbit distortions induced by the IDs are also investigated, starting from measurements performed on the existing SOLEIL storage ring and followed by an analysis of their impact on the SOLEIL II lattice.

FOCUSING AND COUPLING EFFECTS

Characteristics of Phase 1 IDs

At the current stage, among the three IDs whose designs differ from those of SOLEIL, only the kick map of the newly designed 5-meter-long APU (APU250) has been updated in the simulations. The kick maps of all other IDs are still based on existing SOLEIL devices, but with smaller minimum gaps to better reproduce the expected operating conditions of Phase 1 of SOLEIL II. For each helical-type undulator, four polarization modes are investigated, namely linear tilted (LT), linear horizontal (LH), linear vertical (LV), and circular (CR) modes.

Assuming a worst-case scenario in which all IDs operate at their minimum gaps and all helical-type undulators are

set to the same polarization mode, the ID-induced focusing and coupling effects on the bare lattice were simulated. As shown in Table 2, the reduction in Touschek lifetime is significant compared with that of the bare lattice (3.5 h), particularly in the LT mode, where additional betatron coupling is generated even with ideal ID magnetic fields.

Table 2: Focusing and Coupling Effects of all Phase 1 IDs on the SOLEIL II Bare Lattice under Uniform Polarization Mode for Helical-Type Undulators

Parameter	Modes			
	LT	LH	LV	CR
$\Delta\nu_x$	+0.0053	+0.0107	-0.0272	-0.0114
$\Delta\nu_y$	+0.0459	+0.0325	+0.0556	+0.0460
β_x-beating [%]	2.6	2.6	2.8	2.0
β_y-beating [%]	3.3	3.0	4.1	3.3
Add. coupling [%]	0.06	0	0	0
Touschek lifetime [h]	2.6	2.7	2.7	3.3

Global LOCO Correction

To confirm the feasibility of operating all IDs in the SOLEIL II storage ring, the recovery ability of the Touschek lifetime was evaluated using a global LOCO correction scheme. The LOCO correction was performed within the MATLAB-based `AT` environment using the `Toolkit for Simulated Commissioning (SC)` [21]. The whole orbit response matrix, together with dispersion, were included in the objective function. All available quadrupole correctors, including 372 normal quadrupole (QN) correctors and 134 skew quadrupole (QT) correctors, were used as fitting variables to compensate for the ID-induced focusing and coupling effects. The BPM noise was introduced according to the SOLEIL II error model [22]. After four iterations, the obtained corrector strengths were applied to recover the nominal optics.

The lattice parameters after the global LOCO correction in the four polarization modes are summarized in Table 3. After correcting the tune shifts, beta-beating, and additional coupling, the Touschek lifetime was recovered to values close to or above 3.3 h, which is acceptable for operation.

Table 3: Parameters in Presence of all Phase 1 IDs after Global LOCO Correction

Parameter	Modes			
	LT	LH	LV	CR
$\Delta\nu_x$	-0.0003	-0.0004	+0.0008	+0.0003
$\Delta\nu_y$	+0.0005	+0.0009	+0.0006	+0.0006
β_x-beating [%]	0.7	0.4	1.0	0.5
β_y-beating [%]	1.3	1.0	1.8	1.3
Add. coupling [%]	0.004	0	0	0
Max. int. grad. QN [T]	0.03	0.03	0.04	0.02
Max. int. grad. QT [T]	0.04	0	0	0
Touschek lifetime [h]	3.3	3.4	3.3	3.4

Local Correction for Feedforward Compensation

In real machine operation, using LOCO to generate feedforward tables for ID compensation is not considered at the current stage. The main difficulty is that variations in ID gap or phase would require coordinated feedforward corrections applied to power supplies distributed around the entire storage ring, which is challenging to implement in practice. Therefore, a local correction scheme is instead investigated as a more feasible approach.

For each ID, after inserting its second-order kick map into the corresponding straight section, four upstream and four downstream normal quadrupole correctors (with one additional corrector on each side for the APU250) are used to correct the focusing effect. The matching segment extends from the center of the upstream nearest arc bend to that of the downstream one. The Twiss parameters, including the phase advance, at the entrance and exit of the matching segment are matched to those of the bare lattice, while enforcing zero alpha functions at the center of the straight section to preserve lattice symmetry. For each ID exhibiting additional coupling effects in LT mode, two upstream and two downstream skew quadrupole correctors are used for compensation. Finally, 233 out of 372 normal quadrupole correctors are selected as fast correctors under the vacuum chamber cut-off-frequency constraint, split into two families, and used for global tune correction.

The beta-beating before and after applying the global LOCO correction or the local correction, with all the Phase 1 IDs set to LT mode, is shown in Fig. 1. According to the parameters listed in the first column of Table 4, the tune shifts, beta-beating, and coupling after correction are reduced to levels comparable to those obtained with LOCO. Consequently, the Touschek lifetime is also recovered to 3.3 h.

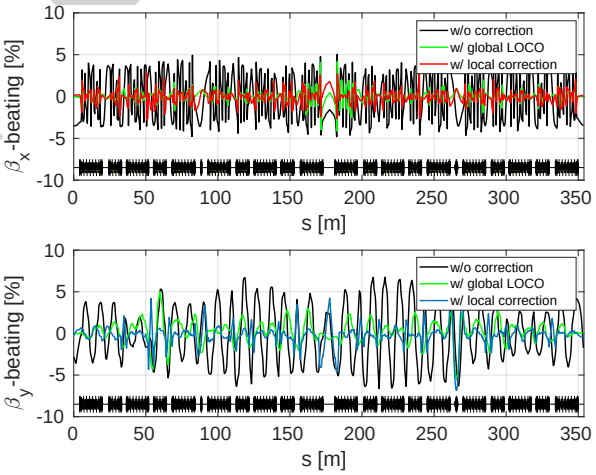

Figure 1: Horizontal (top) and vertical (bottom) beta-beating before and after applying either global LOCO correction or local correction, with all Phase 1 IDs in LT mode.

The results for the other three modes show similar behavior, as summarized in the last three columns of Table 4, further demonstrating the feasibility of this local correction scheme for feedforward ID compensation. However,

the maximum integrated gradient of the normal quadrupole correctors reaches 0.44 T for compensating the IVW. Considering the hardware limit of 1 T, further optimization remains necessary.

Table 4: Parameters in Presence of all Phase 1 IDs after Local Correction for each ID

Parameter	Modes			
	LT	LH	LV	CR
$\Delta\nu_x$	+0.0002	+0.0002	+0.0001	+0.0001
$\Delta\nu_y$	+0.0001	+0.0001	+0.0001	+0.0001
β_x-beating [%]	0.7	0.4	0.6	0.5
β_y-beating [%]	1.2	0.9	1.1	1.0
Add. coupling [%]	0.003	0	0	0
Max. int. grad. QN [T]	0.44	0.44	0.44	0.44
Max. int. grad. QT [T]	0.11	0	0	0
Touschek lifetime [h]	3.3	3.3	3.1	3.2

CLOSED-ORBIT DISTORTION

Measurements on SOLEIL

The ID-induced closed-orbit distortion originates from deviations between the ideal and real magnetic fields. As a result, this effect cannot be directly reproduced using the ideal kick maps implemented in the lattice model. Therefore, measurements of the closed-orbit distortions generated by each type of ID were performed on the SOLEIL storage ring. The measured distortions were then fitted using horizontal and vertical kicks located at the upstream and downstream ID feedforward corrector positions. The RMS fitting error was at the level of 10^{-3} mm. The fitted kicks were subsequently tested on SOLEIL by applying the corresponding currents directly to the feedforward correctors instead of using the original feedforward tables. A significant reduction of the residual closed-orbit distortions was observed after applying the fitted kicks, because the original feedforward tables have not been updated for several years, as the fast orbit feedback system is sufficiently effective during operation. An example for an IVU is shown in Fig. 2. These results demonstrate that the proposed method provides an effective approach for characterizing the closed-orbit distortions generated by the existing IDs.

Compensation Scheme for SOLEIL II

By implementing the fitted kicks in the SOLEIL II lattice, the closed-orbit distortions induced by each ID can be evaluated for the upgraded machine. Fig. 3 compares the distortions generated by the same IVU in SOLEIL and SOLEIL II. Owing to the lower beta functions at the straight-section center of this IVU in SOLEIL II ($\beta_x = \beta_y = 1.4$ m), compared with those in SOLEIL ($\beta_x = 13.8$ m, $\beta_y = 3.0$ m), the resulting distortions are reduced in both transverse planes.

Work has now started on defining the feedforward tables for the existing SOLEIL II Phase 1 IDs, while the locations of

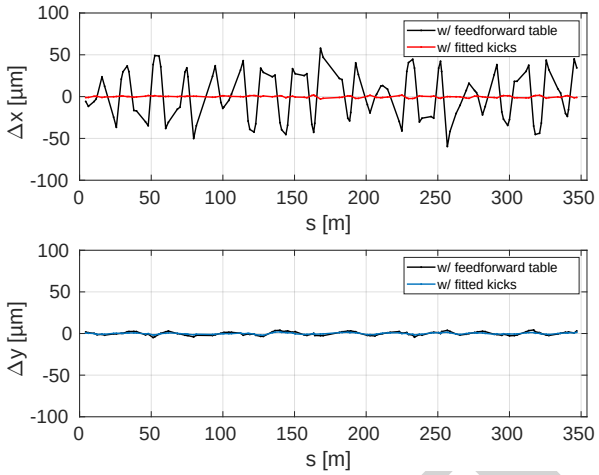

Figure 2: Horizontal (top) and vertical (bottom) residual closed-orbit distortions induced by an IVU on SOLEIL, corrected using either original feedforward table or fitted kicks.

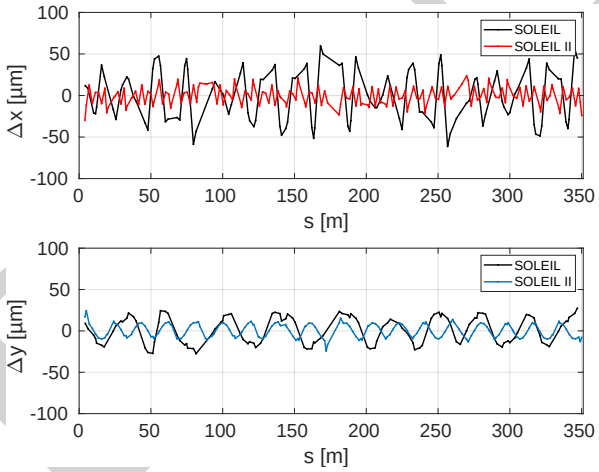

Figure 3: Horizontal (top) and vertical (bottom) closed-orbit distortions induced by an IVU on SOLEIL and SOLEIL II.

their feedforward correctors are being determined. In parallel, given the reduced closed-orbit distortions in SOLEIL II, the capability of the orbit feedback system alone to compensate for such distortions, together with the required feedback response speed, will be evaluated for each type of ID.

SUMMARY AND OUTLOOK

Preliminary studies of the ID compensation scheme for SOLEIL II demonstrate the feasibility of developing feedforward systems to correct ID-induced tune shifts, beta-beating, coupling, and closed-orbit distortions. Further work will focus on completing and optimizing the feedforward compensation scheme, as well as evaluating whether the feedback systems alone are sufficient to compensate for the effects induced by each type of ID. These studies will provide useful input for defining the required specifications of the dipole, normal and skew quadrupole corrector power supplies, particularly regarding response speed.

REFERENCES

[1] Synchrotron SOLEIL Facility Website, https://www.synchrotron-soleil.fr

[2] Conceptual Design Report for the SOLEIL Upgrade, https://www.synchrotron-soleil.fr/en/future-soleil-soleil-ii-project

[3] A. Nadji and L. S. Nadolski, "Upgrade project of the SOLEIL accelerator complex", *Synchrotron Radiat. News*, vol. 36, no. 1, pp. 10–15, 2023. doi:10.1080/08940886.2023.2186661

[4] J. Susini *et al.*, "A brief introduction to the Synchrotron SOLEIL and its upgrade programme", *Eur. Phys. J. Plus*, vol. 139, no. 80, 2024. doi:10.1140/epjp/s13360-024-04872-2

[5] A. Loulergue *et al.*, "TDR baseline lattice for SOLEIL II upgrade project", in *Proc. IPAC'24*, Nashville, TN, pp. 1346–1349, May 2024. doi:10.18429/JACoW-IPAC2024-TUPG47

[6] L. S. Nadolski *et al.*, "SOLEIL II project: entrance in the construction phase", in *Proc. IPAC'25*, Taipei, Taiwan, Jun. 2025, pp. 212–215. doi:10.18429/JACoW-IPAC2025-MOPB074

[7] L. S. Nadolski *et al.*, "SOLEIL II: the French 4GLS project - first year of the construction program", presented at IPAC'26, Deauville, France, May 2026, paper TUO2M01, this conference.

[8] C. Benabderrahmane *et al.*, "Commissioning of the first insertion devices at SOLEIL", in *Proc. PAC'07*, Albuquerque, NM, pp. 929–931, Jun. 2007. doi:10.1109/PAC.2007.4440938

[9] B. Singh *et al.*, "Impact of insertion devices on Diamond-II lattice", in *Proc. IPAC'22*, Bangkok, Thailand, pp. 539–542, Jul. 2022. doi:10.18429/JACoW-IPAC2022-MOPOTK037

[10] B. Singh *et al.*, "Further progress with alternative optics for the Diamond-II storage ring upgrade", in *Proc. IPAC'25*, Taipei, Taiwan, Jun. 2025, pp. 623–626. doi:10.18429/JACoW-IPAC2025-MOPS017

[11] K. Manukyan *et al.*, "The effect of insertion devices on beam dynamics for Elettra 2.0", in *Proc. IPAC'23*, Venice, Italy, pp. 3321–3324, May 2023. doi:10.18429/JACoW-IPAC2023-WEPL094

[12] A. Gamelin *et al.*, "Double RF system design for normal conducting passive harmonic cavity in SOLEIL II", presented at IPAC'26, Deauville, France, May 2026, paper WEP5092, this conference.

[13] Y. Huang *et al.*, "Study of gas scattering–induced beam losses and collimation for the SOLEIL II storage ring", presented at IPAC'26, Deauville, France, May 2026, paper TUP2617, this conference.

[14] O. Marcouille *et al.*, "Panoply of insertion devices for SOLEIL II", *Journal of Physics: Conference Series*, vol. 3010, no. 1, p. 012010, 2025. doi:10.1088/1742-6596/3010/1/012010

[15] M. Couprie *et al.*, "The SOLEIL II insertion devices", presented at IPAC'26, Deauville, France, May 2026, paper THP2152, this conference.

[16] O. Chubar, P. Elleaume, and J. Chavanne, "A three-dimensional magnetostatics computer code for insertion devices", *Journal of Synchrotron Radiation*, vol. 5, no. 3, pp. 481–484, 1998. doi:10.1107/S0909049597013502

[17] A. Terebilo, "Accelerator modeling with MATLAB Accelerator Toolbox", in *Proc. PAC'01*, Chicago, IL, pp. 3203–3205, Jun. 2001. doi:10.1109/PAC.2001.988056

[18] S. White, L. Carver, L. Farvacque, and S. Liuzzo, "Status and recent developments of python Accelerator Toolbox", in *Proc. IPAC'23*, Venice, Italy, pp. 3185–3188, Sep. 2023. doi:10.18429/JACoW-IPAC2023-WEPL031

[19] P. Elleaume, "A new approach to the electron beam dynamics in undulators and wigglers", in *Proc. EPAC'92*, Berlin, Germany, pp. 661–664, Mar. 1992. https://proceedings.jacow.org/e92/PDF/EPAC1992_0661.PDF

[20] J. Safranek, "Experimental determination of storage ring optics using orbit response measurements", *Nucl. Instrum. Meth. A*, vol. 388, pp. 27–36, 1997. doi:10.1016/S0168-9002(97)00309-4

[21] T. Hellert, P. Amstutz, C. Steier, and M. Venturini, "Toolkit for simulated commissioning of storage-ring light sources and application to the advanced light source upgrade accumulator", *Phys. Rev. Accel. Beams*, vol. 22, no. 10, p. 100702, 2019. doi:10.1103/PhysRevAccelBeams.22.100702

[22] S. Habet *et al.*, "Start to end commissioning simulations for SOLEIL II storage ring", in *Proc. IPAC'25*, Taipei, Taiwan, Jun. 2025, pp. 698–701. doi:10.18429/JACoW-IPAC2025-MOPS040